Energy Engineering

Tech Science Press

Doi:10.32604/ee.2025.062844

ARTICLE

Characterizing and Stage-Wise Differentiation of Coal Spontaneous Combustion in Deep Mines

Haitao Wang[1,2,*], Pengxin Zhang[2], Weihao Li[2], Baogang Li[1] and Xianghui Xiong[1]

[1]School of Resources and Engineering Department, Heilongjiang University of Technology, Jixi, 158100, China
[2]Intelligent Mine Interdisciplinary Research Institute, Heilongjiang University of Science & Technology, Harbin, 150022, China
*Corresponding Author: Haitao Wang. Email: wht820718@163.com

Received: 29 December 2024; Accepted: 20 February 2025; Published: 31 March 2025

ABSTRACT: Deep mining, characterized by high stress, elevated geothermal gradients, and significant moisture content, significantly increases the risk of Coal Spontaneous Combustion (CSC), posing a major threat to mine safety. This study delves into the impact of these factors on the self-ignition properties of coal, leveraging data from four distinct mines in Heilongjiang Province, China: Shuangyashan Dongrong No. 2 Mine, Hegang Junde Coal Mine, Qitaihe Longhu Coal Mine, and Jixi Ronghua No. 1 Mine. We have honed the theoretical framework to account for variations in gas content during CSC. Our investigation, conducted through programmed temperature rise experiments, scrutinized the generation and temperature-dependent evolution of gases, emphasizing individual indicators such as CO, O_2, and C_xH_y, in addition to composite indicators like the ratio of change in CO to change in O_2 concentration ($\frac{\partial C_{CO}}{\partial t}:-\frac{\partial C_{O_2}}{\partial t}$) and the ratio of C_2H_4 to C_2H_6. These insights have catalyzed the development of a CSC state energy level transition model and a precise method for phase-based quantification of combustion progression. Our findings furnish a scientific foundation for the formulation of early warning and prevention strategies in deep mining settings.

KEYWORDS: Deep mine; coal spontaneous combustion; gas change rate; index threshold

1 Introduction

By 2022, China's coal reserves totaled 207.012 billion tons, accounting for 67.4% of the nation's energy production [1]. Coal continues to be the most plentiful and strategically vital energy resource within the country [2]. Nonetheless, the spontaneous combustion of coal has consistently ranked as a paramount safety hazard in coal mining, with statistics revealing that over 85% of coal mine fires originate from spontaneous combustion within coal seams. Moreover, the depth of coal mining in China is progressing subterraneously at a pace of no less than 10 m per annum, progressively escalating the intricacy of mining deep coal seams.

2 Analysis of the Effects of Deep Mine Characteristics

2.1 Effects of High Stress on CSC

High stress significantly affects coal's spontaneous combustion characteristics by altering its physical structure and mechanical properties [3–6]. Under such conditions, the coal body's fracture system is prone to expansion, accompanied by a significant rise in fracture density and porosity. These fractures facilitate oxygen diffusion into the coal, permitting oxygen molecules to infiltrate deeper into coal particles and substantially increasing the apparent rate of coal oxidation. The increase in microcracks also amplifies the number of reactive sites on the coal surface, offering additional areas for oxygen adsorption and chemical reactions.

Moreover, high stress leads to localized stress concentration areas within the coal body, which intensifies the release of internal energy and shortens the induction period of oxidation. Local deformation can further accelerate gas emissions from the coal seam, allowing oxygen concentrations around the coal body to more readily attain the critical levels necessary for oxidation reactions.

2.2 Effects of High Geothermal Gradient on CSC

The high-temperature environment in deep mines enhances the reactivity of active functional groups in coal molecules, enabling oxidation reactions at lower temperatures. Under such thermal conditions, the thermal decomposition of coal is hastened, and the heat generated from oxidation reactions tends to accumulate within the coal mass rather than dissipate. Empirical studies have demonstrated that once the geothermal gradient surpasses 150°C, the rate of coal oxidation escalates exponentially, markedly elevating the risk of spontaneous combustion [7–9].

2.3 Effects of High Moisture on CSC

Coal in high-moisture environments exhibits distinct self-ignition characteristics compared to dry conditions [10,11]. The presence of moisture modifies the coal's pore structure, augmenting the reactivity of the pore surfaces. Moreover, moisture contributes an additional source of heat during the adsorption and desorption processes, thereby fostering oxidation reactions. Elevated moisture levels also influence the thermal conductivity of coal, facilitating the accumulation of heat within the coal mass and consequently heightening the susceptibility to spontaneous combustion.

2.4 Synergistic Effects of High Stress, High Geothermal Gradient, and High Moisture

The combined effects of high stress, high geothermal gradients, and high moisture levels complicate coal's spontaneous combustion characteristics [12,13]. High stress intensifies fractures, thereby promoting oxygen diffusion and reactions; high geothermal gradients expedite the kinetics of oxidation reactions; and high moisture levels alter the thermophysical properties of coal, impeding the effective dissipation of heat generated by oxidation. The synergistic impact of these factors substantially amplifies the risk of CSC within deep mines (as depicted in Fig. 1).

The complexity of deep mining environments increases the challenges associated with preventing and managing coal spontaneous combustion (CSC). Accurate assessment of the risk levels of CSC in deep mines is fundamental for effective fire prevention, while monitoring the type and concentration changes of environmental gases in flammable zones is a critical means of predicting self-ignition risks [14–16]. Wang et al. [17], through a combination of experiments and on-site testing of characteristic gases, identified CO and C_2H_4 as the main marker gases in the goaf of the Longtan Coal Mine. Yang et al. [18], based on natural fire experiments in the Dafosi Coal Mine, confirmed C_2H_4 as a key indicator gas for CSC. Furthermore, Hao et al. [19] proposed that, based on the varying gas indicator weights during the stages of slow oxidation, accelerated oxidation, and intense oxidation, C_2H_6, CO, and C_2H_2 can be used as marker gases for the initial, middle, and later stages, respectively. Wang et al. [20] investigated the characteristics of various combustible gases produced during the spontaneous combustion of long-flame coal and their impact on the explosion limits of methane. Wu et al. [21] established a solid-gas-thermal coupled multiphysics model to systematically investigate the spatiotemporal evolution of temperature fields and indicator gas distributions, as well as their dynamic relationships, during the spontaneous combustion process in longwall goaf. Ma et al. [22] investigated the generation characteristics of combustible gases during lignite oxidation using a programmed temperature gas testing system, analyzing the effects of particle size and temperature. The results indicate that gas production is significantly influenced by particle size

above 200°C, with CO dominating in the early stages, while CH_4 and H_2 increase notably after 300°C. Li et al. [23] conducted a study on the stages of coal spontaneous combustion using differential scanning calorimetry and programmed temperature experiments, and applied the grey correlation method to calculate the correlation between heat release intensity and gas product concentrations under different oxygen concentrations. The research revealed that the low-temperature oxidation process of coal can be divided into three stages: rapid endothermic, slow endothermic, and exothermic. Zhou et al. [24] investigated the residual coal in the goaf of the Z109 working face in the Donggucheng Mine. Through programmed heating experiments, the production of carbon monoxide and hydrocarbon gases during coal oxidation was measured, and the variation characteristics of gas ratios with temperature were further analyzed. The coal spontaneous combustion process was subdivided into seven stages, and a quantitative composite parameter-based early warning system for coal spontaneous combustion classification was established. Liu et al. [25] analyzed the multi-scale evolution patterns based on wavelet transform to determine the evolution processes, periodic distributions, and correlations of CO and O_2 volume fractions in different regions, thereby evaluating the susceptibility of these regions to coal spontaneous combustion. It was determined that the CO and O_2 volume fractions in the working face exhibit multi-scale effects, demonstrating periodic variations across different time scales.

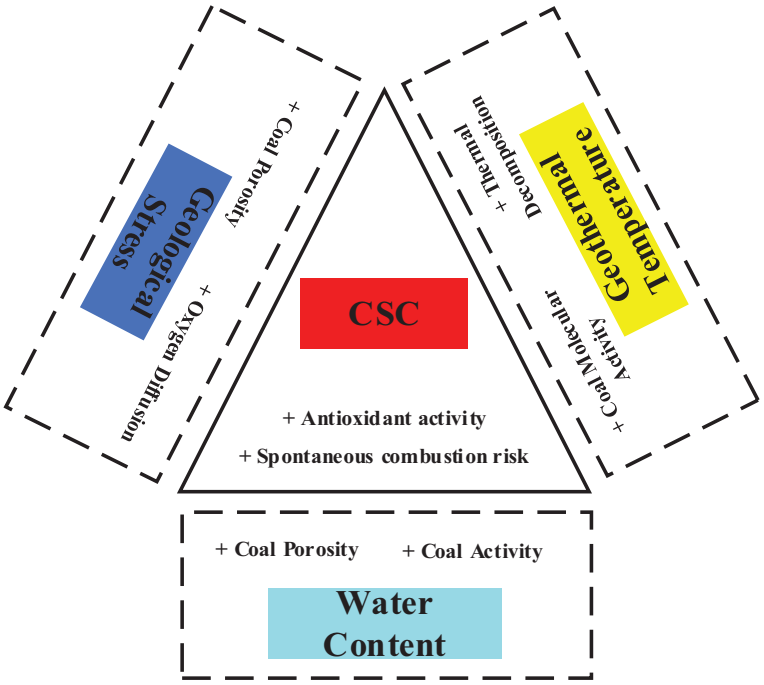

Figure 1: The effects of high stress, high geothermal gradient, and high moisture on CSC characteristics

Presently, research pertaining to early warning systems for CSC in deep mines faces certain constraints, particularly in the realm of marker gas selection and the adaptability of predictive models. This study zeroes in on the distinctive conditions of deep-mined coal seams in Heilongjiang Province, delving into the characteristics of CSC and instituting an early warning indicator system. A tiered indicator system, predicated on individual gas indicators, composite indicators, and gas growth rate analysis, is presented. This system provides theoretical and practical insights that facilitate the early prediction of spontaneous combustion within deep coal seams.

3 Experiment

3.1 Coal Sample Selection

Coal samples were collected from four mining regions in Heilongjiang Province: Shuangyashan Dongrong No. 2 Mine (DR), Hegang Junde Mine (JD), Qitaihe Longhu Mine (LH), and Jixi Ronghua No. 1 Mine (RH). These mines, which adopt vertical shaft development and exhaust ventilation methods, have immediate roofs and floors predominantly composed of shale or mudstone, while the old roof and floor is typically sandstone or limestone. The mining depth ranges from −300 to −600 m (see Fig. 2).

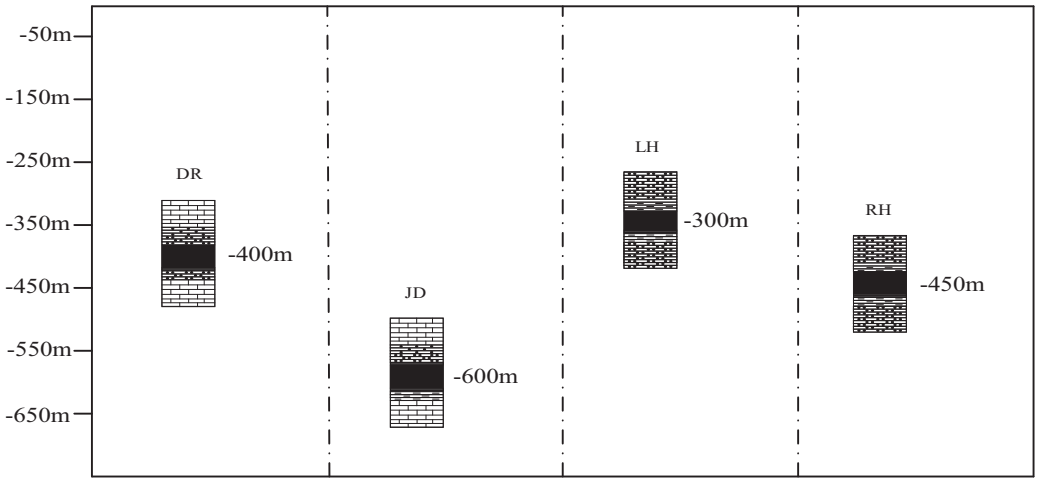

Figure 2: Coal sample collection sites

These regions, with their varied geological settings and coal types, provide a robust regional representation and scientific relevance. Post-extraction, the coal samples were dispatched to the Fire Prevention Laboratory at Heilongjiang University of Science and Technology for comprehensive proximate and elemental analysis. A detailed breakdown of the analytical outcomes for each coal sample is presented in Table 1.

Table 1: Experimental results of coal industry, elements analysis and porosity

Coal samples	Coal Types	Mad	Aad	Vad	FCad	Cad	Had	Oad	Nad	Sad	P
DR	Long-flame coal	2.65	12.80	41.02	43.53	68.00	2.80	12.05	1.50	0.20	7.53%
JD	Gas coal	2.65	15.88	39.68	41.79	83.16	5.65	8.57	2.31	0.31	8.21%
LH	1/3 coking coal	1.94	13.55	25.65	58.86	85.60	5.38	7.32	1.23	0.47	2.85%
RH	Coking coal	2.23	14.38	31.28	52.11	87.69	4.89	6.04	1.02	0.36	3.26%

3.2 Coal Sample Preparation

Raw coal samples were crushed under ambient pressure and sieved. These samples were categorized into five distinct particle size fractions using laboratory sieves: 0–1.0 mm, 1.0–3.0 mm, 3.0–6.0 mm, 6.0–9.0 mm, 9.0–13.0 mm, maintaining an equal proportion of 1:1:1:1:1 for each fraction. The sieved coal samples were homogeneously mixed to form a 1 kg batch of coal samples with a blended particle size. The prepared samples were then properly sealed and stored for future experimental use.

3.3 Experimental Setup and Methods

The experiments were conducted using a programmed temperature rise testing apparatus developed by Heilongjiang University of Science and Technology. The apparatus consists of three main components: a gas flow control system, a temperature-controlled chamber, and a gas collection and analysis module (see Fig. 3). The experimental procedure is as follows:

- The mixed coal samples were carefully loaded into the reaction vessel, which was then sealed to maintain experimental integrity.
- The sealed reaction vessel was placed in the temperature-controlled chamber, and preheated air was introduced into the reaction vessel from the bottom through the gas flow system, with the gas flow precisely controlled by a flowmeter. Referring to the large-scale coal spontaneous combustion experimental platform of Xi'an University of Science and Technology, the air flow rate was set to 120 mL/min in proportion.
- The temperature-controlled chamber controlled the temperature inside the reaction vessel according to the preset temperature rise program, gradually increasing from ambient temperature to 200°C at a rate of 1°C/min. Four constant temperature stages were set: the first stage at 60°C for 30 min, the second stage at 100°C for 60 min, and the third stage at 160°C for 90 min.
- Gas samples were collected at the top of the reaction vessel through a sampling device under different coal temperature conditions. Once the coal temperature reached 30°C, gas samples were collected from the outlet of the storage tank, with one sample taken every 10°C increase.
- The collected gas samples were analyzed using a gas chromatograph to determine the composition and concentration of the gases. The main gases tested included CO, O_2, C_2H_6, and C_2H_4, to assess the oxidation of coal samples and the changes in gas generation during the heating process.
- The entire experiment lasted approximately 8 h. To ensure the accuracy of the experimental results, each group of experiments was repeated 3 to 5 times, and the average value was taken as the final data.

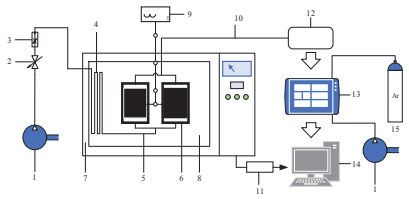

1—Air Compressor; 2—Pressure Reducing Valve; 3—Flow Meter; 4—Gas Preheater; 5—Intake Pipe; 6—Reactor Vessel; 7—Insulation Layer; 8—Coal Sample Oxidation Chamber; 9—Thermometer; 10—Exhaust Pipe; 11—Temperature Acquisition System; 12—Gas Collection Dryer; 13—Gas Chromatograph; 14—Computer; 15—Carrier Gas

(a)

(b)

Figure 3: Temperature programmed system (a) schematic diagram of the temperature-programmed system; (b) photograph of the temperature-programmed system

3.4 Theoretical Analysis of Gas Content Variation

Coal temperature serves as a pivotal parameter for gauging the advancement of coal spontaneous combustion (CSC). The sensitivity of individual gas indicators can be compromised by myriad interference factors, resulting in divergences between inferred characteristic temperatures and actual conditions. To bolster the precision of predictions, a gas concentration variation formula has been formulated in

this study. This formula takes into account variables such as coal's pore structure, ambient temperature, and humidity levels, expanding upon the gas variation rate methodology presented in existing literature [26–29]. The formula leverages fluctuations in pivotal gas indicators—namely CO, O_2, and C_2H_4—to deduce coal temperature and appraise the stage of combustion. By juxtaposing the Graham fire coefficient against composite gas indicators, this study refines the selection of gas indicators across pivotal temperature thresholds, diminishing the dependency on single gas indicators and markedly improving the reliability of predictive models.

(1) Theoretical Formula for O_2 Consumption

The diffusion of oxygen from the mine environment into coal pores follows Fick's First Law of Diffusion:

$$J_{O_2} = -D_e \frac{\partial C_{O_2}}{\partial x} \tag{1}$$

$$D_e = D_0 \times \varphi^n \times \tau \times f(T, P) \tag{2}$$

$$D_0 = D_{O_2}^{ref} \times \left(\frac{T}{T_{ref}}\right)^{\frac{3}{2}} \times \frac{P_{ref}}{P} \tag{3}$$

$$f(T, P) = e^{\left(-\frac{Ea}{RT}\right)} \tag{4}$$

where

J_{O_2}: Oxygen diffusion flux (mol/m^2·s).

D_e: Effective diffusion coefficient, influenced by factors such as pore structure, temperature, and pressure.

$\frac{\partial C_{O_2}}{\partial x}$: Oxygen concentration gradient within coal pores.

$D_{O_2}^{ref}$: Molecular Diffusion Coefficient of Oxygen under Standard Conditions.

T: Actual temperature.

T_{ref}: Reference temperature.

P: Actual pressure.

P_{ref}: Reference pressure.

ϕ: Coal porosity.

n: Porosity index.

τ: Porosity tortuosity.

$f(T, P)$: Comprehensive correction function for temperature and pressure.

Ea: Rate of oxygen consumption (mol/m^3·s).

R: Universal gas constant (8.314 J/(mol·K)).

The rate of reaction between oxygen and active functional groups on the coal surface is represented as:

$$R_o = k_s C_{O_2} \times e\left(-\frac{E_a}{RT}\right) \tag{5}$$

where

R_o: Oxygen Chemical Reaction Rate.

k_s: Reaction Rate Constant.

Considering both diffusion and chemical reaction, by combining Eqs. (1)–(5), the rate of oxygen consumption is:

$$\frac{dC_{O_2}}{dt} = -D_e \frac{\partial^2 C_{O_2}}{\partial x^2} - k_s C_{O_2} \times e^{\left(-\frac{Ea}{RT}\right)} \tag{6}$$

(2) The Rate of Gas Generation from CSC

R_g represents the rate of generation of gases (such as CO, CH_4, C_xH_y, etc.) during the spontaneous combustion of coal, which is proportional to the rate of chemical reaction with oxygen:

$$R_g = \eta R_{O_2} = \eta k_s C_{O_2} \times e^{\left(-\frac{E_a}{RT}\right)} \tag{7}$$

where

R_g: the rate of gas.

H: the efficiency factor, indicating the proportion of gas generated in the chemical reaction with oxygen.

The diffusion process of the generated gas conforms to Fick's second law of diffusion.

$$\frac{\partial C_g}{\partial t} = D_e \frac{\partial^2 C_g}{\partial x^2} \tag{8}$$

By combining Eqs. (6)–(9), the formula for the generation of gas from coal spontaneous combustion is derived:

$$\frac{\partial C_g}{\partial t} = D_e \frac{\partial^2 C_g}{\partial x^2} + \eta k_s C_{O_2} \times e^{\left(-\frac{E_a}{RT}\right)} \tag{9}$$

4 Experimental Results and Analysis

4.1 Analysis of Single Gas Indicator Variations

Programmed temperature rise experiments were conducted on coal samples from four deep mining regions. The findings revealed that the predominant byproducts during the initial, low-temperature oxidation phase were carbon monoxide (CO), methane (CH_4), and carbon dioxide (CO_2). With an escalation in coal temperature, ethane (C_2H_6) and ethylene (C_2H_4) correspondingly demonstrated notable and consistent alterations.

(1) CO Concentration Variation

Fig. 3a delineates the correlation between CO production and coal temperature across the four coal samples. The concentration of CO escalated exponentially alongside the increasing temperature, with the DR coal sample recording the highest CO levels, succeeded by RH, and LH presenting the lowest. These variations are predominantly ascribed to the low metamorphic degree, elevated volatile content, and the prevalence of oxygen-containing functional groups within the coal samples from deep mining, rendering them more susceptible to oxidative reactions.

During the initial phase of the experiment, each coal sample yielded a measurable quantity of carbon monoxide (CO) as a result of low-temperature oxidation initiated during the crushing and loading processes. With the progression of temperature, the concentration of CO escalated gradually, manifesting a pattern indicative of distinct stages. As depicted in Fig. 3b, within the temperature range of 60°C–80°C, the rate of CO production for all four coal samples arrived at its first critical inflection point, marking an initial peak in CO concentration. This observation implies a significant intensification in the interaction between coal and oxygen.

Upon further elevation of temperature, there was a marked increase in CO concentration. The DR, RH, and JD coal samples achieved a second peak at 120°C. Later on, the RH, JD, and LH samples showed a third peak at 160°C, 150°C, and 190°C, respectively, while the DR sample's third peak was observed at 180°C. These peaks are aligned with the coal's fracture temperatures, mirroring the stages at which the reactivity of the functional groups within the coal molecules notably amplified.

The correlation analysis between the rate of CO production and temperature variations suggests that the temperature points at which there is a significant increase in CO concentration can be employed as pivotal indicators to delineate the stages of coal oxidation. This finding furnishes a theoretical foundation for the phase-based categorization and early warning mechanisms in the context of coal spontaneous combustion (CSC). If the caption extends over multiple lines, the text should be justified to align with both margins. For a visual reference, refer to Fig. 4.

(2) O_2 Concentration Variation

The correlation between oxygen (O_2) consumption and coal temperature across the four coal samples is illustrated in Fig. 5.

As shown in Fig. 4a, within the temperature range of 30°C–60°C, the consumption of oxygen (O_2) remains minimal, signifying the relative stability of the coal's properties and a correspondingly low risk of spontaneous combustion. This phase is indicative of the slow oxidation stage, during which changes in O_2 consumption are gradual and do not exhibit a significant escalation. Upon reaching temperatures between 60°C–120°C, O_2 consumption commences a gradual increase, yet without intensifying to a marked degree, suggesting the coal samples are transitioning into an intermediate oxidation phase characterized by more vigorous reactions.

Beyond 120°C, there is a precipitous rise in O_2 consumption, coincident with distinct indications of spontaneous combustion, signifying the onset of the rapid oxidation stage. The surge in O_2 consumption during this interval mirrors the increased oxygen requirement of the accelerating combustion process. At temperatures surpassing 200°C, O_2 consumption attains its zenith, heralding the commencement of the intense oxidation stage, where both the rate of combustion and the demand for oxygen experience a sharp ascent.

Fig. 4b delineates that the rate of O_2 consumption across the four coal samples follows an overall upward trajectory with fluctuations as the temperature increases. These fluctuations become more pronounced at temperatures surpassing 120°C. Notably, the DR sample demonstrates peaks at 140°C and 190°C, the RH sample peaks at 180°C, the LH sample at 170°C, and the JD sample at 190°C. These observations suggest that the rate of O_2 consumption variation is a pivotal parameter for delineating the distinct stages of coal spontaneous combustion (CSC).

(3) C_xH_y Concentration Variation

The generation characteristics of ethane (C_2H_6) and ethylene (C_2H_4) during the programmed temperature rise of coal samples from the four mines are shown in Fig. 6.

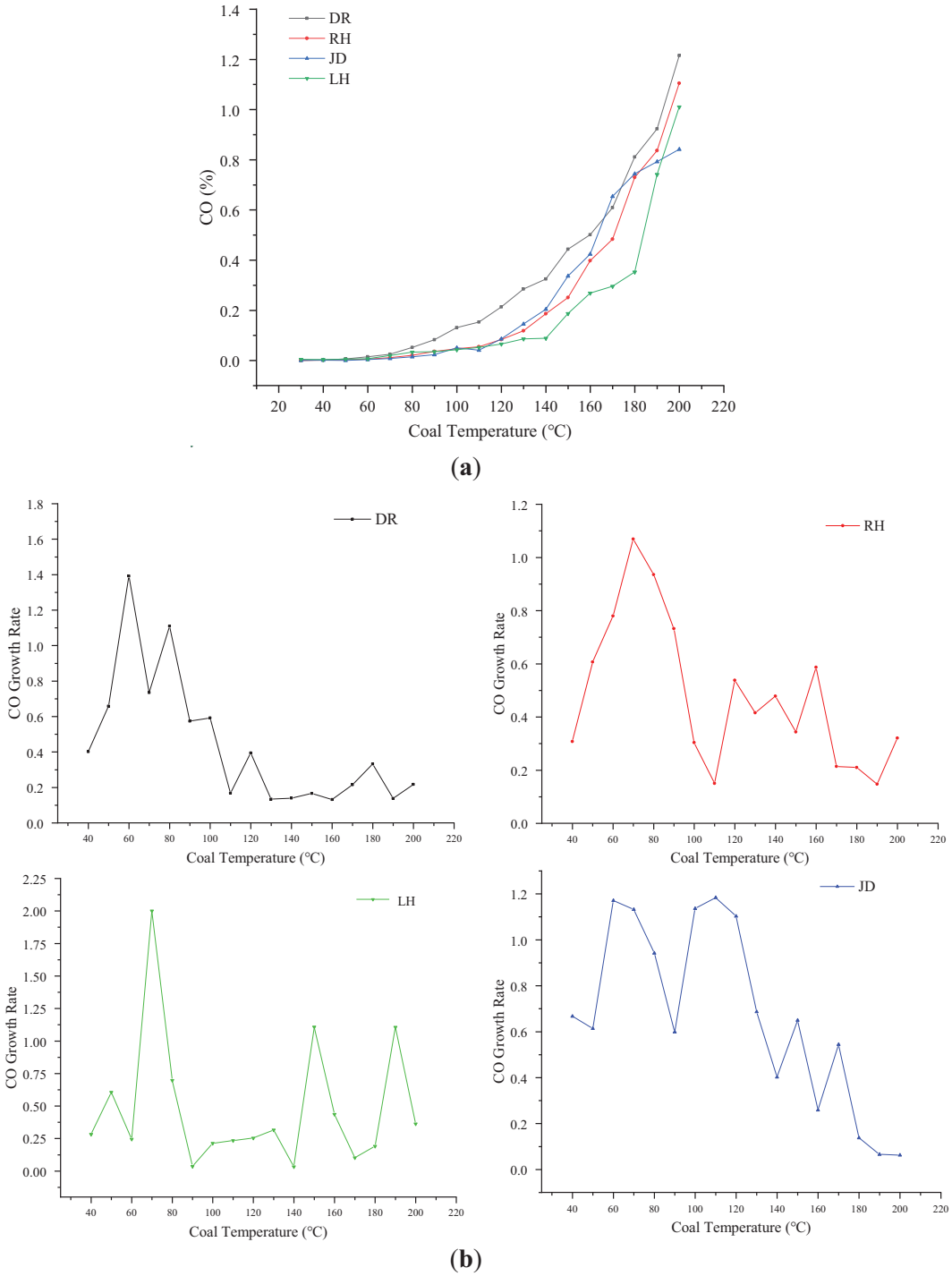

Figure 4: Trends in CO concentration relative to varying coal temperatures. (a) CO concentration; (b) CO concentration change rate

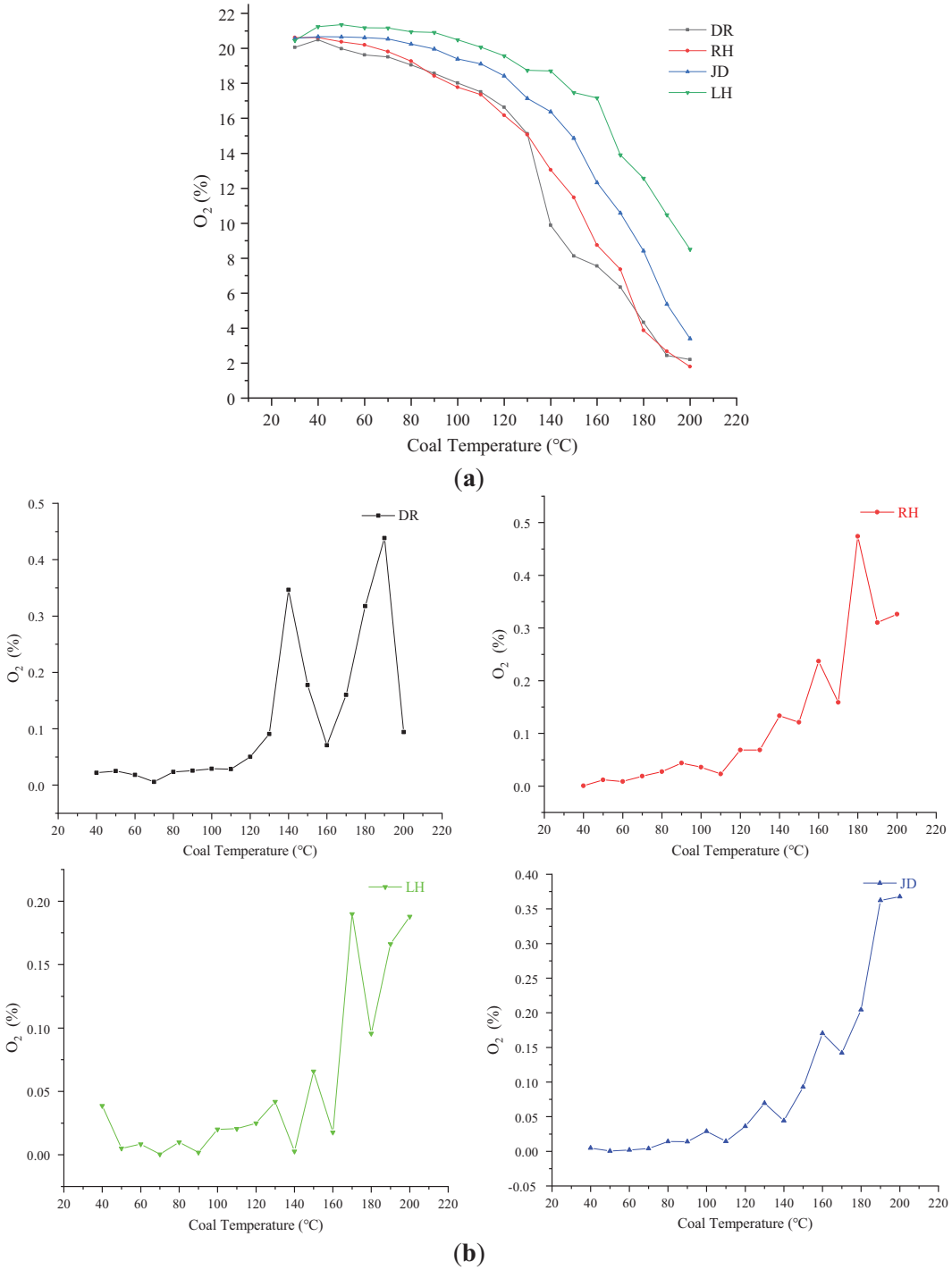

Figure 5: Variation in oxygen concentration as a function of coal temperature. (a) O_2 concentration; (b) O_2 concentration change rate

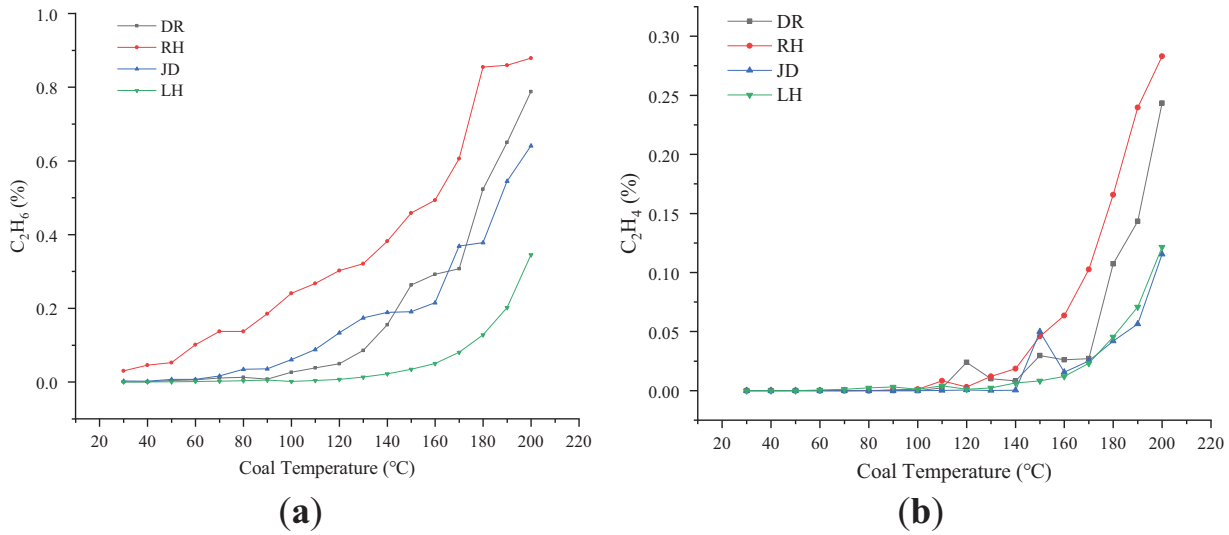

Figure 6: Correlation of hydrocarbon gas (C_xH_y) levels with coal temperature dynamics. (a) C_2H_6 concentration change; (b) C_2H_4 concentration change

From Fig. 6a, it can be observed that the production of C_2H_6 in all mines increases with rising temperature, though variations exist among different mines. In some mines, C_2H_6 generation begins at low temperatures (below 60°C), indicating that temperature is a critical factor influencing C_2H_6 formation. Between 60°C and 120°C, the rate of C_2H_6 production accelerates, suggesting enhanced coal spontaneous combustion activity. In the range of 120°C to 200°C, C_2H_6 generation increases significantly, reflecting the transition to an intense oxidation stage and a heightened risk of C_2H_6 formation. Specifically:

(a) For the DR coal sample, C_2H_6 generation is relatively low at low temperatures but rises sharply above 120°C.
(b) The RH coal sample exhibits a significantly higher C_2H_6 generation rate starting at 60°C compared to other samples.
(c) The JD coal sample shows a rapid increase in C_2H_6 production after 80°C.
(d) The LH coal sample initially exhibits slow C_2H_6 generation, but the rate accelerates markedly beyond 120°C.

From Fig. 6b, it is evident that C_2H_4 production also increases significantly with temperature, further demonstrating its strong temperature dependence. The initial temperatures for C_2H_4 generation vary among the mines:

(a) The DR coal sample shows limited C_2H_4 production even at high temperatures, indicating a higher threshold temperature for C_2H_4 formation.
(b) The RH coal sample begins generating C_2H_4 at relatively low temperatures (around 60°C), but the production rate does not increase significantly at higher temperatures.
(c) The JD coal sample exhibits a notable increase in C_2H_4 generation rate at higher temperatures, resulting in higher overall production.
(d) The LH coal sample initiates C_2H_4 generation at a lower temperature threshold with a relatively fast initial rate, though the maximum production level remains constrained.

These experimental findings suggest that the generation patterns of C_2H_6 and C_2H_4 can serve as distinctive indicators for various stages of CSC. The analysis of their production quantities and rates in

relation to temperature yields vital data for refining CSC monitoring and early warning systems, thereby enhancing the precision and timeliness of predictions.

4.2 Analysis of Composite Gas Index Changes

(1) Characteristics of $\frac{\partial C_{CO}}{\partial t}:-\frac{\partial C_{O_2}}{\partial t}$

The characteristics of $\frac{\partial C_{CO}}{\partial t}:-\frac{\partial C_{O_2}}{\partial t}$ during the programmed temperature rise of coal samples from four mines are shown in Fig. 7.

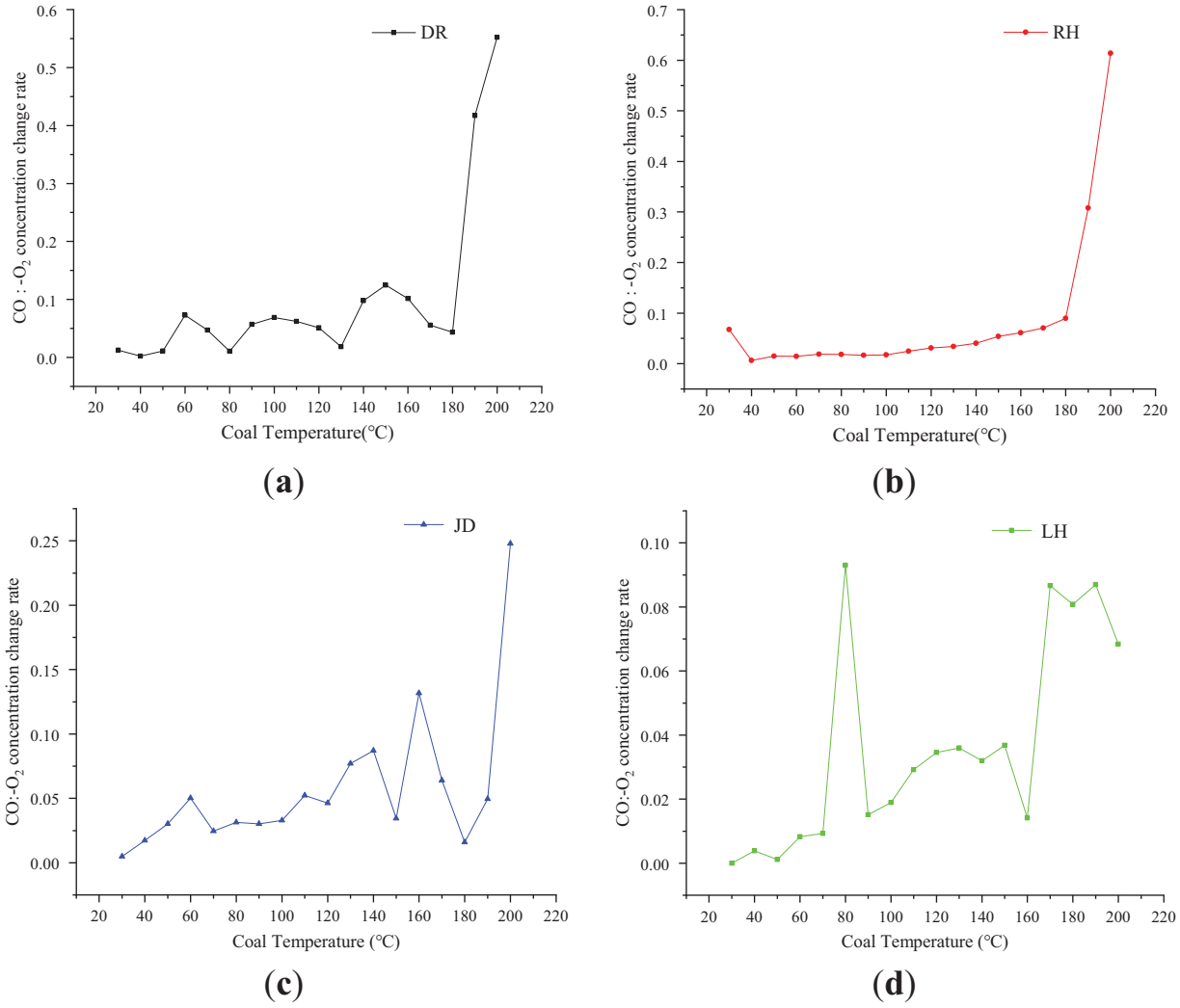

Figure 7: Relationship between CO: -O_2 concentration change rate and coal temperature. (a) Relationship between CO: -O_2 concentration change rate and temperature in DR; (b) Relationship between CO: -O_2 concentration change rate and temperature in RH; (c) Relationship between CO: -O_2 concentration change rate and temperature in JD; (d) Relationship between CO: -O_2 concentration change rate and temperature in LH

As illustrated in Fig. 7, the ratio of CO to O_2 concentration change rates displayed distinct trends in response to temperature variations across the different coal samples:

DR and RH Coal Samples: The ratio exhibited minor fluctuations at temperatures below 180°C, suggesting a relatively subdued oxidation reaction in the coal. However, beyond 180°C, the ratio increased dramatically, indicating the transition to a rapid oxidation stage where the production rate of CO significantly exceeded the consumption rate of O_2. JD Coal Sample: The ratio demonstrated significant fluctuations below 180°C, yet these were of limited extent. Above 180°C, the ratio increased markedly, implying an enhanced reactivity of the functional groups within the coal molecules. LH Coal Sample: A peak in the ratio was observed at 80°C, potentially due to the accelerated reaction rates of specific active functional groups at this temperature. Beyond 160°C, the ratio increased significantly, indicative of rapid oxidation, although the overall trend was less uniform.

Despite the differences in the ratio among the coal samples, the DR, RH, and JD samples showed relatively consistent patterns during spontaneous combustion, with notable increases beyond critical temperatures, such as 180°C. These ratios are crucial parameters for identifying the stages of coal oxidation. Conversely, the LH sample showed less consistency, but the general trend still mirrored the progressive nature of coal oxidation. These observations indicate that the ratio of CO to O_2 concentration change rates is a valuable indicator for monitoring coal spontaneous combustion (CSC) and classifying its stages, thus enhancing the accuracy of early warning systems.

(2) Characteristics of C_2H_4:C_2H_6

The behavior of the C_2H_4:C_2H_6 ratio throughout the programmed temperature increase of the coal samples is depicted in Fig. 8.

As presented in Fig. 8, an upward trend in the C_2H_4:C_2H_6 ratio with increasing temperatures was observed across all coal samples. This trend indicates that the concentration of C_2H_4 increased more significantly relative to C_2H_6, which is a characteristic feature of coal gasification processes. Despite minor variations in the ratio among different coal samples, the general trends were strikingly consistent:

DR Coal Sample: The ratio reached its maximum at 120°C, followed by a sharp decline and a subsequent gradual recovery. Below 100°C, no C_2H_4 was detected, resulting in a ratio of zero within this temperature range. RH Coal Sample: The ratio showed a significant increase post 100°C, achieving its first peak at 110°C. Beyond 140°C, the ratio experienced a sharp increase and continued to rise. LH Coal Sample: The ratio began to rise at 50°C, peaked sharply at 110°C, and then declined rapidly. Beyond 120°C, the ratio increased gradually. JD Coal Sample: The ratio reached its peak at 150°C, followed by a sharp decrease and a slow recovery. Below 100°C, no C_2H_4 was detected, and the ratio showed minor fluctuations between 100°C and 150°C.

These experimental findings underscore that the generation patterns of C_2H_6 and C_2H_4 can serve as distinctive indicators for various stages of coal spontaneous combustion (CSC). The analysis of their ratio variations and trends offers crucial data for refining the monitoring and early warning systems for coal combustion, thereby enhancing the accuracy and timeliness of predictions.

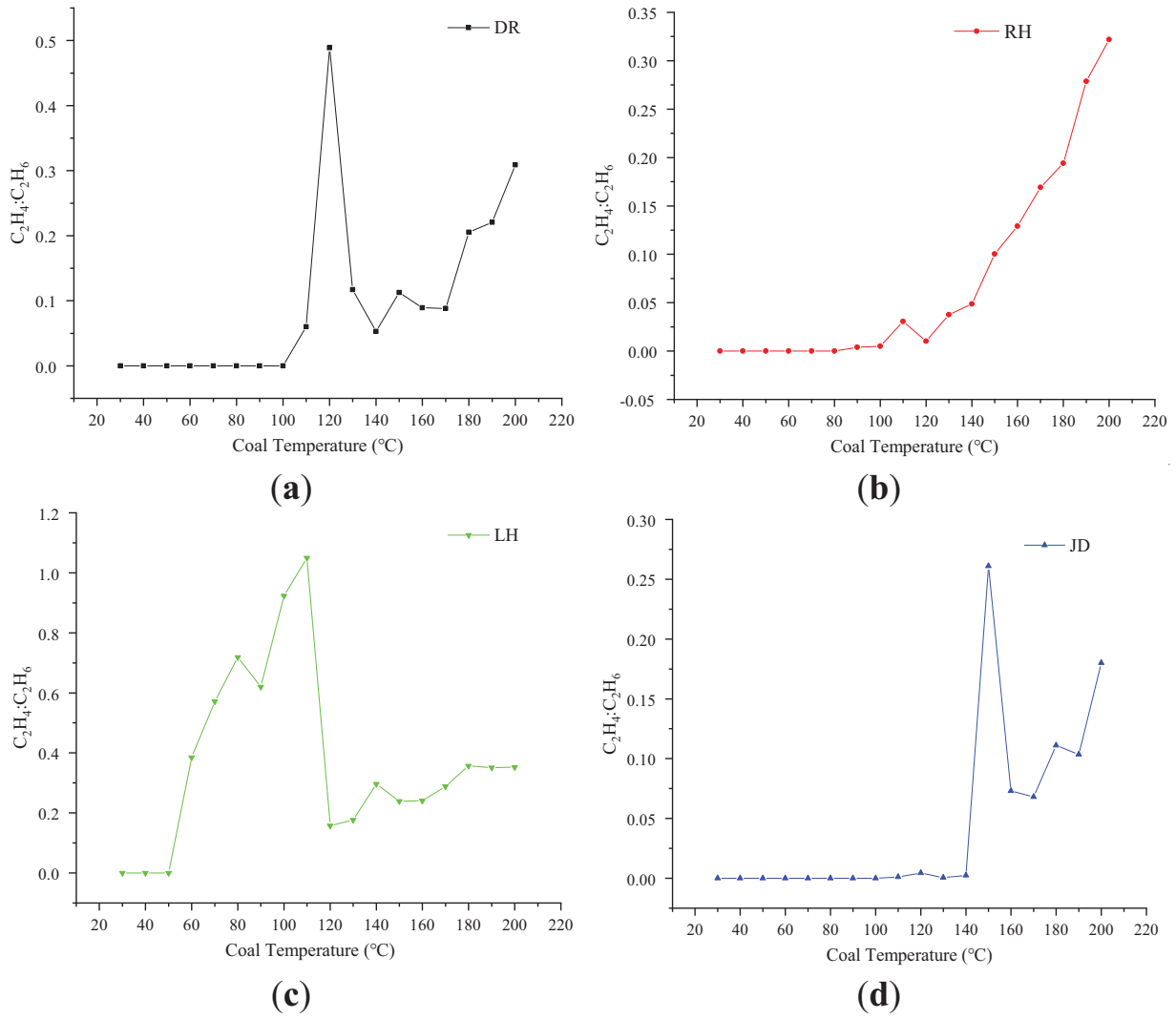

Figure 8: Changes in the C_2H_4 to C_2H_6 ratio across different coal temperature ranges. (a) Variation of C_2H_4:C_2H_6 ratio in DR with temperature; (b) Variation of C_2H_4:C_2H_6 ratio in RH with temperature; (c) Variation of C_2H_4:C_2H_6 ratio in LH with temperature; (d) Variation of C_2H_4:C_2H_6 ratio in JD with temperature

5 CSC Stage Classification

Classifying CSC stages and providing early warnings depend on identifying critical temperatures. Drawing on data from programmed temperature rise experiments and integrating principles from coal-oxygen composite kinetics, quantum chemistry, and thermodynamics, while considering the temperature characteristics of CSC in deep mines, the stages of CSC have been delineated. A spatial distribution model and an energy-level transition model for CSC states have been developed (refer to Fig. 9). The process is categorized into five distinct stages across four characteristic temperature ranges.

Experimental data from coal samples extracted from mines in Heilongjiang revealed that the ignition point was rapidly attained once the temperature of the coal exceeded 200°C. In alignment with the principles of fire prevention and control for coal spontaneous combustion (CSC), the temperature stages were classified with a focus on temperatures below 200°C. Characteristic temperature thresholds were used to delineate the process into five distinct stages, as detailed in Table 2.

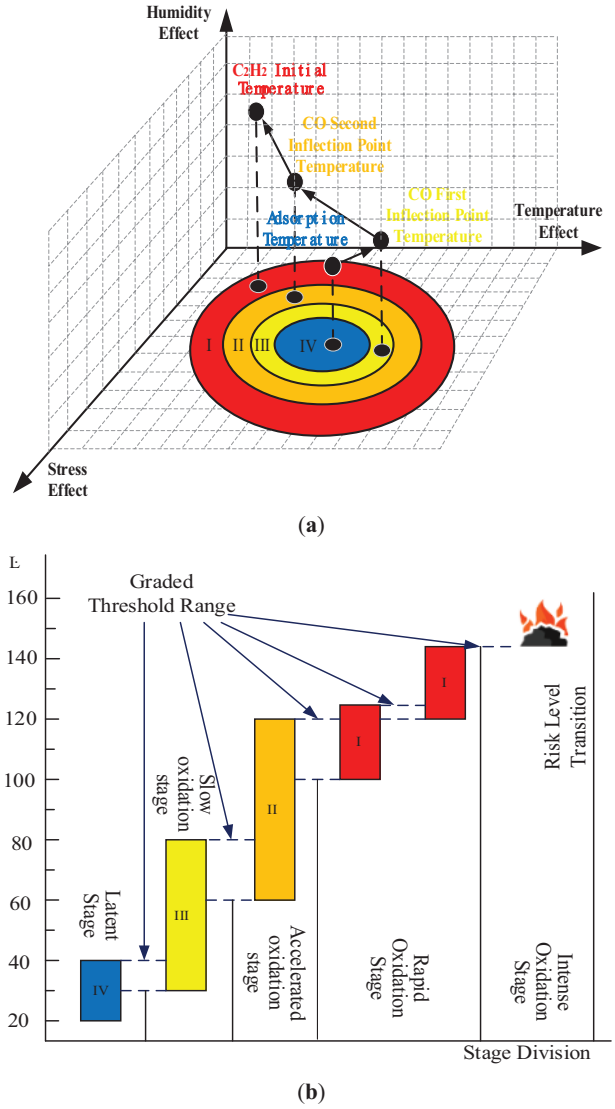

Figure 9: Division of CSC stage. (a) Spatial distribution of CSC state transition; (b) Energy level transition of CSC state

Table 2: Division of CSC process

Grade	Spontaneous combustion stage	Temperature range	Characteristic parameters	Index
IV	Latent stage (Below adsorption temperature)	From 20°C to 30°C–40°C	The CO generation and $\frac{\partial C_{CO}}{\partial t}$ increase. The C_{O_2} experiences a slight decrease, leading to an acceleration in the reaction rate.	$\{C_{O_2} > 20\% \cap \frac{\partial C_{O_2}}{\partial t} < 0.02\} \cap \{C_{CO} < 10 \times 10^{-6}\%\} \cap \{C_{C_2H_4} = 0\} \cap \{C_{C_2H_6} = 0\}$
III	Slow oxidation stage (Adsorption temperature to critical temperature)	From 30°C–40°C to 60°C–80°C	The CO generation increases significantly, and the $\frac{\partial C_{CO}}{\partial t}$ reaches a peak. The C_{O_2} is relatively steady. Peaks are observed in the ratios of $\frac{\partial C_{CO}}{\partial t}$:$-\frac{\partial C_{O_2}}{\partial t}$ and C_2H_4:C_2H_6.	$\{C_{O_2} \in (18\sim20)\% \cap \frac{\partial C_{O_2}}{\partial t} < 0.02\} \cap \{C_{CO} \in (10\sim100) \times 10^{-6}\%\} \cap \{C_{C_2H_4} = 0\} \cap \{C_{C_2H_6} = 0\}$
II	Accelerated oxidation stage (Critical temperature to dry cracking temperature)	From 60°C–80°C to 100°C–120°C	The CO generation accelerates, with the $\frac{\partial C_{CO}}{\partial t}$ peaking. The C_{O_2} declines more rapidly, and the $\frac{\partial C_{O_2}}{\partial t}$ peaks. Small amounts of C_2H_4:C_2H_6 are produced, with the C_2H_4:C_2H_6 ratio peaking.	$\{C_{O_2} \in 16\sim18\% \cap C_{CO} \in (100\sim600) \times 10^{-6}\%\} \cap \{C_{C_2H_6} \in (0\sim20) \times 10^{-6}\% \cup C_{C_2H_4} \in (0\sim20) \times 10^{-6}\%\}$
I	Rapid oxidation stage (Dry cracking temperature to pyrolysis temperature)	From 100°C–120°C to 160°C–180°C	The CO generation increases rapidly, with $\frac{\partial C_{CO}}{\partial t}$ peaking. C_{O_2} declines quickly, with the $\frac{\partial C_{O_2}}{\partial t}$ peaking. A certain amount of C_2H_4 and C_2H_6 is produced.	$\{C_{O_2} \in 5\sim16\% \cap C_{CO} \in (600\sim3500) \times 10^{-6}\%\} \cap C_2H_4$:$C_2H_6$ Maximum $\cap \{C_{C_2H_6} \in (20\sim40) \times 10^{-6}\% \cup C_{C_2H_4} \in (20\sim40) \times 10^{-6}\%\}$

(Continued)

Table 2 (continued)

Grade	Spontaneous combustion stage	Temperature range	Characteristic parameters	Index
Combustion stage	Intense oxidation stage (Above pyrolysis temperature)	Above 180°C	The CO generation increases sharply, while the $\frac{\partial C_{CO}}{\partial t}$ remains relatively stable. The decline in C_{O_2} is relatively gentle, and the $\frac{\partial C_{O_2}}{\partial t}$ peaks. A large amount of C_2H_4 and C_2H_6 is produced, with the C_2H_4:C_2H_6 ratio reaching an extreme value.	$\{C_{O_2} < 5\% \cap \{C_{CO} > 3500\ \text{ppm}\} \cap \{C_{C_2H_6} > 40 \times 10^{-6}\% \cup C_{C_2H_4} > 40 \times 10^{-6}\%\}$

6 Conclusions

(1) The study identified significant trends in single and composite gas indicators during the CSC process. Through the analysis of gas variation rates, the study examined changes in the concentration and growth rate of carbon monoxide (CO), the concentration and consumption rate of oxygen (O_2), and the concentrations of hydrocarbon gases (C_xH_y). Key indicators, such as the ratio of change in CO to change in O_2 concentration and the ratio of ethylene (C_2H_4) to ethane (C_2H_6), were identified. It was determined that, based on characteristic temperatures, the spontaneous combustion process of coal seams in Heilongjiang Province can be categorized into five distinct stages: the latent stage (20°C to 30°C–40°C), slow oxidation stage (30°C–40°C to 60°C–80°C), accelerated oxidation stage (60°C–80°C to 100°C–120°C), rapid oxidation stage (100°C–120°C to 160°C–180°C), and intense oxidation stage (above 180°C). Thresholds for early warning indicators for each stage were also established.

(2) The study demonstrated that the combined effects of high stress and high geothermal gradients significantly increased the risk of CSC in deep mines. Experimental results showed consistent trends in spontaneous combustion among coal samples from different mines under similar conditions, despite variations in specific combustion temperatures and gas generation amounts. Within the coal temperature range of 30°C to 200°C, the generation rates and amounts of different gases exhibited distinct patterns. The generation of CO, C_2H_4, and C_2H_6 increased with temperature, reaching peaks at specific temperature intervals. The generation and consumption rates of CO, O_2, and C_xH_y, along with temperature-related rapid growth points, were identified as key indicators for distinguishing coal oxidation stages. Indicators such as the ratio of change in CO to change in O_2 concentration, the ratio of C_2H_4 to C_2H_6, and gas concentration variation rates effectively supported stage classification.

(3) Building on the theoretical framework of CSC stages and monitoring methods, this study enhanced the early warning threshold system. By integrating characteristic temperatures and gas generation patterns, multiple approaches-including single gas indicators, composite indicators, and gas variation rates-were adopted to optimize the early warning system for CSC, thereby improving the accuracy of predictions.

(4) The CSC state energy level transition model and phase-based quantification method developed in this study can be applied in mining operations as follows: By monitoring the changes in coal temperature and gas indicators, combined with the model and method proposed in this study, early signs of coal spontaneous combustion can be identified in a timely manner, thus allowing for preemptive measures to prevent the occurrence of spontaneous combustion accidents. Corresponding preventive measures can be taken according to different stages of coal spontaneous combustion. During the mine design phase, the findings of this study can be referred to for the rational planning of the mining sequence and ventilation system of the mine, so as to reduce the risk of coal spontaneous combustion. In the process of mine management, the model and method of this study can be used to dynamically assess the risk of coal spontaneous combustion in the mine, and to adjust the mining and management strategies in a timely manner.

(5) While this study has made significant progress in characterizing and stage-wise differentiating CSC in deep mines, there are still some limitations. For example, this study mainly focuses on the impact of deep mine environmental factors such as high stress, high geothermal gradient, and high humidity on the characteristics of coal spontaneous combustion, but does not fully consider the impact of other potential factors, such as bacterial activity and the specific surface area of coal. Bacterial activity may affect the spontaneous combustion process by promoting the biological oxidation of coal, and the specific surface area of coal will affect its contact area with oxygen, thereby affecting the rate of oxidation reaction. Future research can further explore the impact of these factors on the characteristics of coal spontaneous combustion to more comprehensively understand the mechanism of coal spontaneous combustion in deep mines.

Acknowledgement: The authors acknowledge the support from Intelligent Mine Interdisciplinary Research Institute, Heilongjiang University of Science & Technology, Harbin, China.

Funding Statement: This paper is supported by "Unveiling the List and Leading the Way" Science and Technology Research Project from Heilongjiang Province (2021ZXJ02A03); Major Science and Technology Support Action Plan for the "Millions" Project in Heilongjiang Province (2020ZX04A01) and the Natural Science Foundation of Heilongjiang Province (LH2024E112).

Author Contributions: The authors confirm contribution to the paper as follows: Conceptualization and methodology by Haitao Wang; writing—review and editing by Pengxin Zhang and Weihao Li; writing—original draft preparation by Baogang Li and Xianghui Xiong. All authors reviewed the results and approved the final version of the manuscript.

Availability of Data and Materials: This data available on request from the authors.

Ethics Approval: Not applicable.

Conflicts of Interest: The authors declare no conflicts of interest to report regarding the present study.

References

1. Ministry of Natural Resources, PRC. China mineral resources. Beijing, China: Geological Press; 2023.
2. International Energy Agency. Coal 2023 analysis and forecast to 2025. Paris, France: IEA; 2023.
3. Pan R, Ma Z, Yu M, Chao J, Li C, Wang J. Study on the mechanism of coal oxidation under stress disturbance. Fuel. 2020;275(6):117901. doi:10.1016/j.fuel.2020.117901.
4. Chu T, Wu C, Jiang B, Zhu T, Zhang X, Chen Y, et al. Low-temperature oxidation characteristics and apparent activation energy of pressurized crushed coal under stress loading. Nat Resour Res. 2024;299(12):1–13. doi:10.1007/s11053-024-10444-z.

5. Chao J. Experimental study on oxidative spontaneous combustion characteristics of loaded crushed coal [dissertation]. Jiaozuo, China: Henan Polytechnic University; 2019.
6. Thabari JA, Auzani AS, Nirbito W, Muharam Y, Nugroho YS. Modeling of coal spontaneous fire in a large-scale stockpile. Int J Technol. 2023;14(2):257. doi:10.14716/ijtech.v14i2.5367.
7. Hu D, Pan R, Chao J, Jia H, Liu W. Spontaneous combustion characteristics of hydrothermal erosion coal from deep mining and its microscopic mechanism. Energy. 2025;314(2):134268. doi:10.1016/j.energy.2024.134268.
8. Ma DJ, Tang YB. Microstructural evolution of coal under high-temperature oxidation. Energy. 2020;213(2):118800. doi:10.1016/j.energy.2020.118800.
9. Jia H, Yang Y, Ren W, Kang Z, Shi J. Experimental study on the characteristics of the spontaneous combustion of coal at high ground temperatures. Combust Sci Technol. 2022;194(14):2880–93. doi:10.1080/00102202.2021.1895775.
10. Liu X, Dong K, Zhang Y, Duan M, Lu Z, Wang J. Thermodynamic characterization and spontaneous combustion mechanism of coal in continuous hot-humid air flow. Energy. 2025;317(2):134702. doi:10.1016/j.energy.2025.134702.
11. Qu GY, Deng J, Ren SJ, Wang CP, Song ZY, Wang JR, et al. Research on temperature measurement model of loose coal considering humidity using acoustic wave method. Fuel. 2024;373(6):132317. doi:10.1016/j.fuel.2024.132317.
12. Niu HY, Sun QQ, Bu YC, Chen HY, Yang YX, Li SP, et al. Study of the microstructure and oxidation characteristics of residual coal in deep mines. J Clean Prod. 2022;373(10):133923. doi:10.1016/j.jclepro.2022.133923.
13. Zhang J. Study on the evolution mechanism of spontaneous combustion behavior of deep pre-oxidized coal [master's thesis]. Ganzhou, China: Jiangxi University of Science and Technolog; 2023.
14. Wang K, Hu L, Deng J, Zhang Y. Multiscale thermal behavioral characterization of spontaneous combustion of pre-oxidized coal with different air exposure time. Energy. 2023;262(1):125397. doi:10.1016/j.energy.2022.125397.
15. Adamus A, Šancer J, Guřanová P, Zubiček V. An investigation of the factors associated with interpretation of mine atmosphere for spontaneous combustion in coal mines. Fuel Process Technol. 2011;92(3):663–70. doi:10.1016/j.fuproc.2010.11.025.
16. Wojtacha-Rychter K, Smoliński A. A study of dynamic adsorption of propylene and ethylene emitted from the process of coal self-heating. Sci Rep. 2019;9(1):18277. doi:10.1038/s41598-019-54831-6.
17. Wang Y, Zhou Y. Critical gas indicators for spontaneous combustion in coal seams. Fire Saf J. 2023;141:103956. doi:10.1016/j.firesaf.2023.103956.
18. Yang Y, Fei J, Luo Z, Wen H, Wang H. Experimental study on characteristic temperature of coal spontaneous combustion. J Therm Anal Calorim. 2023;148(19):10011–9. doi:10.1007/s10973-023-12365-0.
19. Hao TX, Zhang LL, Li F, Wang ZH. Optimization of coal spontaneous combustion marker gas based on principal component analysis. Coal Technol. 2023;42(10):176–81. doi:10.13301/j.cnki.ct.2023.10.040.
20. Wang H, Liu Y, Shan Q. Influence of gas from long-flame coal spontaneous combustion on gas explosion limit. Int J Chem Eng. 2023;2023(1):5096109. doi:10.1155/2023/5096109.
21. Wu X, Si G, Jing Y, Yu Z, Ren T, Mostaghimi P. Indicator gases under thermal effect in a multiphysics coupling model of longwall goaf during coal self-heating. Appl Therm Eng. 2025;264:125513. doi:10.1016/j.applthermaleng.2025.125513.
22. Ma D, Zhu T, Yuan P, Zhang L. Study on the characteristics of combustible mixed gas production during lignite oxidation process. Fire. 2024;7(10):367. doi:10.3390/fire7100367.
23. Ren LF, Yu X, Li QW, Tao F, Weng TF, Zhai XW, et al. Thermodynamic characteristics of weakly caking coal oxidation and variation law of gaseous products in low oxygen concentration environment. Case Stud Therm Eng. 2024;62:105171. doi:10.1016/j.csite.2024.105171.
24. Zhou Q, Mao X, Jia B. Development of a graded early warning index system and identification of critical temperatures for coal spontaneous combustion using composite gas characteristics. ACS Omega. 2024;9(33):35515–25. doi:10.1021/acsomega.4c02481.
25. Liu X, Wang H, Wang E, Li Z, Liu X, Wang K. Research on evolution law of index gases produced by the coal spontaneous combustion based on wavelet analysis. Fuel. 2024;370(1):131859. doi:10.1016/j.fuel.2024.131859.
26. Chen Q, Qu H, Liu C, Xu X, Wang Y, Liu J. Spontaneous coal combustion temperature prediction based on an improved grey wolf optimizer-gated recurrent unit model. Energy. 2025;314(15):133980. doi:10.1016/j.energy.2024.133980.

27. Gbadamosi AR, Onifade M, Genc B, Rupprecht S. Analysis of spontaneous combustion liability indices and coal recording standards/basis. Int J Min Sci Technol. 2020;30(5):723–36. doi:10.1016/j.ijmst.2020.03.016.
28. Wang K, Li Y, Zhang Y, Deng J. An approach for evaluation of grading forecasting index of coal spontaneous combustion by temperature-programmed analysis. Environ Sci Pollut Res Int. 2023;30(2):3970–9. doi:10.1007/s11356-022-22529-4.
29. Ren L, Tao F, Weng T, Li Q, Yu X, Zhai X, et al. Thermodynamic characteristics and kinetic mechanism of bituminous coal in low-oxygen environments. Nat Resour Res. 2024;33(5):2299–313. doi:10.1007/s11053-024-10352-2.